Research Report

Constitutive Overexpression of *RAM1* Leads to an Increase in Arbuscule Density in *Brachypodium distachyon*[1[OPEN]]

Lena M. Müller,[2] Lidia Campos-Soriano,[3,4] Veronique Levesque-Tremblay,[3,5] Armando Bravo,[3] Dierdra A. Daniels,[6] Sunita Pathak,[7] Hee-Jin Park,[8] and Maria J. Harrison[9,10]

Boyce Thompson Institute, Ithaca, New York 14853

ORCID IDs: 0000-0002-6036-4514 (L.M.M.); 0000-0002-0814-7934 (L.C.-S.); 0000-0003-3869-045X (A.B.); 0000-0001-8015-7005 (D.A.D.); 0000-0002-2745-0525 (S.P.); 0000-0002-5118-6090 (H-.J.P.); 0000-0001-8716-1875 (M.J.H.)

Arbuscular mycorrhizal (AM) symbiosis is a mutually beneficial association of plants and fungi of the subphylum Glomeromycotina. Endosymbiotic AM fungi colonize the inner cortical cells of the roots, where they form branched hyphae called arbuscules that function in nutrient exchange with the plant. To support arbuscule development and subsequent bidirectional nutrient exchange, the root cortical cells undergo substantial transcriptional reprogramming. *REDUCED ARBUSCULAR MYCORRHIZA1* (*RAM1*), previously studied in several dicot plant species, is a major regulator of this cortical cell transcriptional program. Here, we generated *ram1* mutants and *RAM1* overexpressors in a monocot, *Brachypodium distachyon*. The AM phenotypes of two *ram1* lines revealed that *RAM1* is only partly required to enable arbuscule development in *B. distachyon*. Transgenic lines constitutively overexpressing *BdRAM1* showed constitutive expression of AM-inducible genes even in the shoots. Following inoculation with AM fungi, *BdRAM1*-overexpressing plants showed higher arbuscule densities relative to controls, indicating the potential to manipulate the relative proportion of symbiotic interfaces via modulation of *RAM1*. However, the overexpressors also show altered expression of hormone biosynthesis genes and aberrant growth patterns, including stunted bushy shoots and poor seed set. While these phenotypes possibly provide additional clues about the scope of influence of *BdRAM1*, they also indicate that directed approaches to increase the density of symbiotic interfaces will require a more focused, potentially cell type specific manipulation of transcription factor gene expression.

The GRAS (for GA3 INSENSITIVE [GAI], REPRESSOR OF GAI [RGA], and SCARECROW [SCR]) transcription factor *REDUCED ARBUSCULAR MYCORRHIZA* (*RAM1*) has been characterized in three dicot plant species where it is a major regulator of arbuscular mycorrhizal (AM) symbiosis. In *Medicago truncatula*, *Lotus japonicus*, and *Petunia hybrida ram1* mutants, AM fungi display limited arbuscule branching and reduced hyphal colonization of the root, which results in a nonfunctional symbiosis (Gobbato et al., 2013; Park et al., 2015; Rich et al., 2015; Xue et al., 2015; Pimprikar et al., 2016). *RAM1* expression is induced in colonized cortical cells and is regulated by CYCLOPS, a transcription factor of the common symbiosis signaling pathway (Pimprikar et al., 2016) and also by DELLA proteins (Park et al., 2015; Pimprikar et al., 2016), negative regulators of GA signaling (Davière and Achard, 2013). RNA sequencing of *ram1* mutants (Luginbuehl et al., 2017), as well as smaller scale gene expression analyses of roots overexpressing *RAM1* (Park et al., 2015; Jiang et al., 2017), indicate that RAM1 either directly or indirectly regulates expression of several symbiosis-associated transcription factors, including the GRAS transcription factor *RAD1*, and three AP2-domain transcription factors of the *WRINKLED5* (*WRI5*) family. RAM1 also either directly or indirectly regulates expression of genes involved in the production and transfer of lipids to the fungal symbiont (e.g. *FatM*, *RAM2*, and *STR*) and the phosphate transporter *PT4* (Gobbato et al., 2012; Park et al., 2015; Pimprikar et al., 2016; Luginbuehl et al., 2017; Jiang et al., 2018). However, to date, only one lipid biosynthesis gene, *RAM2*, has been established as a direct target of RAM1 (Gobbato et al., 2012). Regulation of the other lipid biosynthesis and transport genes likely occurs indirectly through the action of *WRI5* family genes (Luginbuehl et al., 2017; Jiang et al., 2018).

RAD1, a GRAS transcription factor very closely related to RAM1 (Supplemental Fig. S1; Park et al., 2015; Xue et al., 2015) is also required for AM symbiosis. In *L. japonicus rad1* mutants, AM fungi display defective arbuscule branching phenotypes reminiscent of those seen in *ram1* (Xue et al., 2015); however, in *M. truncatula rad1*, AM fungi show normal arbuscule branching but reduced colonization levels (Park et al., 2015). In line with this observation, several predicted *RAM1* target genes were induced in colonized *L. japonicus ram1* mutants, but induction was completely abolished in *M. truncatula* and *P. hybrida ram1* (Park et al., 2015; Pimprikar et al., 2016; Luginbuehl et al., 2017; Rich et al., 2017). Thus, there are slight differences in regulation of AM symbiosis genes even between relatively closely related plant species (Pimprikar and Gutjahr, 2018).

Several other GRAS proteins are essential for AM symbiosis, including DELLA/SLR1, a negative regulator

of GA signaling (Floss et al., 2013, 2017; Foo et al., 2013; Yu et al., 2014). In *della* mutants, AM fungi show a severely reduced ability to enter cortical cells, and as a result almost no arbuscules are formed (Floss et al., 2013; Foo et al., 2013; Yu et al., 2014). Arbuscules are ephemeral structures, and the few arbuscules that are formed in *della* mutants display an increased lifespan, indicating that DELLA not only regulates arbuscule formation but also their degradation (Floss et al., 2017). Two other GRAS transcription factors critical for hormone signaling and AM symbiosis are *NSP1* and *NSP2*. These transcription factors regulate phosphate-dependent strigolactone (SL) biosynthesis in *M. truncatula* and rice (*Oryza sativa*; Liu et al., 2011). SLs serve as direct plant communication molecules with AM fungi at the onset of the symbiosis. Mutants impaired in NSP or enzymes required for SL biosynthesis show a reduction in fungal entry into the root and consequently reduced colonization (Gomez-Roldan et al., 2008; Liu et al., 2011; Kobae et al., 2018). Thus, there are several examples of GRAS factors that connect hormone signaling and AM symbiosis.

Many GRAS factors operate in complexes with other GRAS proteins, and emerging evidence suggests that this is also true of those involved in AM symbiosis. *M. truncatula* and *L. japonicus* RAM1 were reported to interact with RAD1 and NSP2 (which also interact with each other), but not NSP1 (Gobbato et al., 2012; Park et al., 2015; Xue et al., 2015; Heck et al., 2016). In addition, rice RAM1 interacts with the GRAS transcription factor DIP1, which in turn interacts with DELLA (Yu et al., 2014). *M. truncatula* DELLA proteins were found to interact with numerous other GRAS transcription factors, including RAD1, MIG1, NSP1, and NSP2 (Floss et al., 2016; Fonouni-Farde et al., 2016; Heck et al., 2016; Jin et al., 2016). While their functional significance for symbiosis remains to be determined, the interactions suggest the existence of interconnected transcriptional modules regulated by multiple GRAS transcription factors.

Brachypodium distachyon is a monocot model species capable of forming AM symbiosis (Hong et al., 2012) and amenable to genetic manipulation (Bragg et al., 2015). A recent study identified 48 GRAS transcription factors in the genome of *B. distachyon* (Niu et al., 2019). Here, we report functional analyses of the GRAS transcription factor *RAM1* in a monocot and assess the potential to alter the levels of symbiotic interfaces by manipulating *RAM1* expression.

RESULTS AND DISCUSSION

We identified *Bradi4g18390* as the single *B. distachyon* homolog of the GRAS transcription factor *RAM1* (Supplemental Fig. S1), a gene that is conserved in AM host plants and missing from nonhosts (Bravo et al., 2016). Similar to orthologous *RAM1* genes of *M. truncatula* (Gobbato et al., 2013; Park et al., 2015), *L. japonicus* (Xue et al., 2015; Pimprikar et al., 2016), and *P. hybrida* (Rich et al., 2015), *B. distachyon RAM1* expression is induced in mycorrhizal roots. Following inoculation with the AM fungus *Diversispora epigaea* (formerly *Glomus versiforme*), *BdRAM1* transcripts increased over time in parallel with increasing colonization of the root system as reported by *D. epigaea α-tubulin* transcripts and the phosphate transporter gene *BdPT7* (Hong et al., 2012), a plant gene marker of AM symbiosis (Fig. 1). However, while the transcriptional patterns mirror the marker genes, it is noticeable that *BdRAM1* transcript levels are low.

The role of *RAM1* in AM has been established in at least three dicot host plants (Gobbato et al., 2013; Park et al., 2015; Rich et al., 2015; Xue et al., 2015; Pimprikar et al., 2016), where it is essential to support arbuscule development and appears to act in the upper tier of a transcription factor hierarchy (Luginbuehl et al., 2017); when ectopically overexpressed in roots, *RAM1* is sufficient to induce expression of several AM-induced genes in the absence of symbiosis (Park et al., 2015; Pimprikar et al., 2016). Given its AM-inducible expression and pivotal regulatory role, we hypothesized that constitutive, high-level expression of *RAM1* might increase the occurrence of arbuscules and possibly overall colonization levels, and this might provide an opportunity to evaluate the functional consequences of modifying colonization patterns. To test this hypothesis, we transformed *B. distachyon* with an overexpression construct, *BdRAM1*, under the control of two copies of the

[1]This work was supported by the U.S. Department of Energy, Office of Science, Office of Biological and Environmental Research (grant no. DE–SC0012460), the TRIAD Foundation, the Swiss National Science Foundation (Early Postdoc.Mobility fellowship to L.M.M.), the German Research Foundation (Postdoctoral Fellowship to L.M.M.), and a Marie Curie Fellowship (grant no. FP7–PEOPLE–2013–IOF–624739 to L.C.-S.).

[2]Present address: Department of Biology, University of Miami, Coral Gables, Florida 33146

[3]These authors contributed equally to the article.

[4]Present address: Center for Research in Agricultural Genomics, 08193 Bellaterra, Barcelona, Spain

[5]Present address: Laurentian Forestry Center, Quebec City, Quebec G1V 4C7, Canada

[6]Present address: Valent Biosciences, Libertyville, Illinois 60048

[7]Present address: Donald Danforth Plant Science Center, Olivette, Missouri 63132

[8]Present address: School of Integrative Plant Sciences, Cornell, Ithaca, New York 14853

[9]Author for contact: mjh78@cornell.edu.

[10]Senior author.

The author responsible for distribution of materials integral to the findings presented in this article in accordance with the policy described in the Instructions for Authors (www.plantphysiol.org) is: Maria J. Harrison (mjh78@cornell.edu).

M.J.H. provided overall conceptualization; L.M.M., L.C.-S., and A.B. provided experimental concepts and design; L.M.M., L.C.-S., A.B., V.L.-T., S.P., D.A.D., and H.J.P. performed experimentation; L.M.M., L.C.-S., A.B., and V.L.-T. analyzed the data; L.M.M., L.C.-S., A.B., and M.J.H. interpreted the data; L.M.M. and M.J.H. prepared the manuscript with input from all authors.

[OPEN]Articles can be viewed without a subscription.

www.plantphysiol.org/cgi/doi/10.1104/pp.20.00997

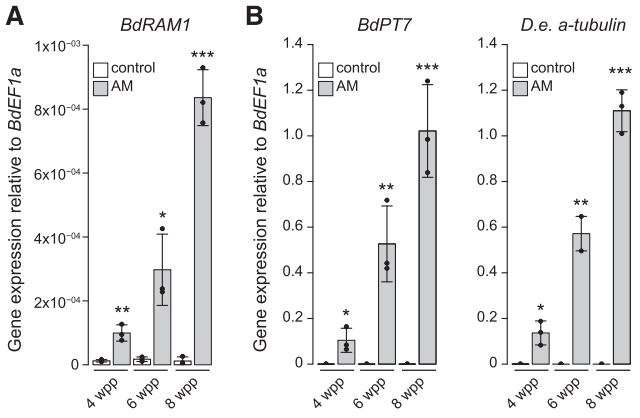

Figure 1. The *B. distachyon* ortholog of *RAM1* is expressed in roots colonized by AM fungi. A, *BdRAM1* gene expression is induced in roots colonized by the AM fungus *D. epigaea* (gray bars) relative to non-mycorrhizal, mock-inoculated roots (white bars). Plants were harvested 4, 6, and 8 weeks postplanting (wpp). AM-induced *BdRAM1* gene expression increases over time. B, Gene expression of the AM marker genes *BdPT7* and *D. epigaea* (*D.e.*) *α-tubulin* in *D. epigaea*-colonized and mock-inoculated control roots over time. A and B, Gene expression was measured by reverse transcription quantitative PCR (RT-qPCR) and normalized to the *B. distachyon* elongation factor *BdEF1α*. Bar graphs show the mean, with error bars representing SD. Single points represent individual measurements. Pairwise comparisons of gene expression in AM and control roots were analyzed separately for each time point using Student's *t* test (***$P < 0.001$, **$P < 0.01$, and *$P < 0.05$).

constitutively active *CaMV 35S* promoter (*35S:BdRAM1*). In addition, we generated *B. distachyon ram1* loss-of-function mutants via CRISPR/Cas9 editing.

Arbuscule Development in *B. distachyon ram1* Mutants Is Partly Impaired

Five independent transgenic lines carrying a two-guide CRISPR/CAS9 construct targeting *BdRAM1* were generated, and two lines in which *BdRAM1* had been edited were chosen for subsequent analysis. In both transgenic lines, the genome had been edited by both guides (Supplemental Fig. S2); editing by the upstream-most guide resulted in premature stop codons and created a truncated protein of 16 amino acids in the first line, designated *ram1-1*. The second line, designated *ram1-2*, was biallelic, with edits resulting in premature stop codons that generated truncated protein products of 16 and 42 amino acids. Both *ram1* lines appeared as wild type with respect to root and shoot morphology.

ram1-1 and *ram1-2* were inoculated with *D. epigaea*, and the fungal colonization patterns were examined after 4 weeks. Some *ram1* roots showed aberrant infection units, reminiscent of the typical dicot *ram1* phenotype, with intraradical hyphae and only small, sparsely branched arbuscules but no fully developed arbuscules (Fig. 2A). However, infection units in other roots of the same plant, or even in other parts of the same root, showed an apparent wild-type morphology with some large, well-branched arbuscules (Fig. 2B). In comparison with the empty vector control, the frequency of aberrant infections in the *B. distachyon ram1* mutants was 2.5- to 3-fold higher, and their overall root colonization levels were 34 to 52% lower. Similar results were obtained in experiments across several generations (Supplemental Fig. S2). These results indicate that *BdRAM1* is required to enable wild-type levels of arbuscule development similar to its orthologs in dicots; however, the *B. distachyon ram1* phenotype is clearly milder than that observed in dicot *ram1* mutants. The finding that *B. distachyon ram1* can support some full arbuscule development suggests that other proteins or pathways have the potential to compensate for loss of *BdRAM1* function. One possible candidate is the GRAS protein *RAD1*, which is closely related to *RAM1* and induced in roots highly colonized by AM fungi (Supplemental Figs. S1 and S3). In legumes, there is evidence of a species-specific micro-diversification of *RAM1* and *RAD1*, with the relative contributions of the two transcription factors to arbuscule development and symbiotic gene expression varying depending on the host species (Park et al., 2015; Xue et al., 2015; Pimprikar et al., 2016; Pimprikar and Gutjahr, 2018). It is therefore conceivable that some diversification of GRAS factor functions has occurred during the evolution of monocots, which might explain the milder arbuscule development phenotype of *B. distachyon ram1* mutants relative to *M. truncatula ram1*. Interestingly, there are other GRAS factor examples where the converse is true, for example the DELLA proteins, where rice *slr* (Yu et al., 2014) shows a stronger phenotype than the *M. truncatula della* double or triple mutants (Floss et al., 2013, 2017). However, in the absence of other monocot *ram1* mutants for comparison, it is also possible that the milder *ram1* phenotype observed here is a feature specific to *B. distachyon*.

Overexpression of *RAM1* Alters Plant Morphology and Results in Constitutive Expression of AM Marker Genes

The generation of transgenic *B. distachyon* plants overexpressing *RAM1* was surprisingly challenging; from two full-scale independent transformation experiments, only three viable independent transgenic *35S:BdRAM1*-overexpressing lines (*35S:BdRAM1^{ox}*) were obtained, and the seed production from these lines was exceedingly poor. In addition, we obtained two lines, which carried the *35S:BdRAM1 T-DNA* but displayed wild type-like *BdRAM1* transcript levels (*35S:BdRAM1^{WT}*). By contrast, transgenic plants carrying *35S:NLS-GFP-GUS* (hereto referred to simply as *35S:NLS-GFP*), were generated without difficulty. Seed production from the latter two genotypes was not impaired.

In addition to poor seed production and viability, the shoot and root phenotypes of the three lines with transcriptional up-regulation of *BdRAM1* (*35S:BdRAM1^{ox}*) differed from the vector controls and from the *35S:BdRAM1^{WT}*

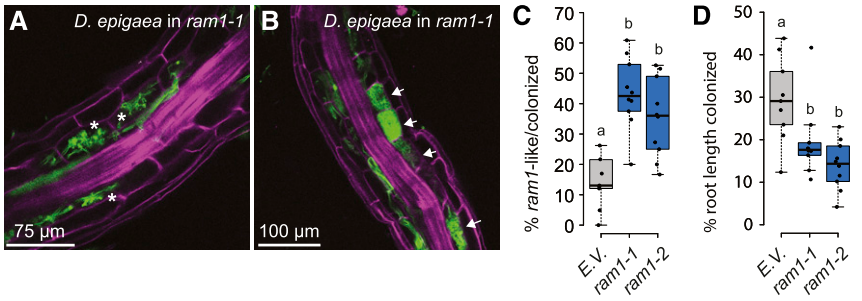

Figure 2. Arbuscule formation is impaired in *B. distachyon ram1* mutants. A, A root piece with *ram1*-like *D. epigaea* arbuscules in CRISPR *ram1* mutants. r*am1*-like infections contain solely arbuscules that are not fully developed and show only sparse branching, reminiscent of the *ram1* mutant phenotype described previously in dicots (indicated by asterisks). B, A root piece with wild type-like *D. epigaea* arbuscules in CRISPR *ram1* mutants. Wild type-like infections contain fully developed arbuscules (indicated by arrows). *D. epigaea* fungal structures visualized using WGA-Alexa Fluor 488 (green), with plant cell walls counterstained using propidium iodide (pink). C, Quantification of *ram1*-like infections relative to the total number of infections in *ram1* CRISPR plants and *B. distachyon* plants transformed with the empty vector (E.V.). The proportion of aberrant infections is increased in two *ram1* alleles (ANOVA, $P = 2.38 \times 10^{-5}$). D, Quantification of total *D. epigaea* root-length colonization in CRISPR *ram1* plants relative to E.V. controls. Root length colonization is significantly decreased in two *ram1* mutant alleles (ANOVA, $P = 0.0014$). Pairwise comparisons in C and D were performed using Tukey's HSD post-hoc test. Different lowercase letters denote significant differences. Box and whisker plots show lower and upper quartiles and minimum and maximum values. The horizontal bar represents the median and the points individual measurements. All results presented in this figure were obtained from the T_3 generation.

plants. The *35S:BdRAM1^{ox}* plants were characterized by a stunted bushy shoot with increased tiller formation and increased leaf angles, as well as a decreased number of node roots (Supplemental Fig. S4). Thus, constitutive overexpression of *BdRAM1* clearly influences plant development. While the cause is unknown, it might be the result of ectopic expression of *BdRAM1* target genes and/or perhaps an interference of RAM1 with other GRAS transcriptional networks, many of which regulate development (for review, see Cenci and Rouard, 2017). Either way, the aberrant developmental phenotypes likely explain the difficulties in regenerating transgenic lines and their fecundity.

The *35S:BdRAM1^{ox}* plants showed constitutive expression of *B. distachyon* orthologs of *RAM2*, *STR*, *PT4*, and *FatM* (Fig. 3A); elevated expression of these genes would normally occur only in response to colonization by AM fungi (for example, Harrison et al., 2002; Paszkowski et al., 2002; Gutjahr et al., 2008, 2012; Zhang et al., 2010; Gobbato et al., 2012; Hong et al., 2012; Bravo et al., 2017), and we observed a similar expression pattern in *B. distachyon* mycorrhizal roots (Fig. 1B; Supplemental Fig. S3). Given the prior knowledge from dicots, we had anticipated that *35S:BdRAM1^{ox}* would increase expression of these genes in roots, but it was surprising to see that expression of these genes was also induced in shoots (Fig. 4). There were some exceptions; expression of *BdSTR* increased in *35S:BdRAM1^{ox}* shoots, but not in roots, while *BdFatM2* showed the opposite expression pattern (Figs. 3A and 4B; Supplemental Fig. S5). Overall, these data indicate that *BdRAM1* alone is sufficient to drive increased expression of these genes in the absence of AM fungi and that transcription cofactors, if required for *Bd*RAM1 function, must be present in all tissues.

In dicots, *RAM1* regulates expression of a second tier of transcription factors including *RAD1* and three members of the *WRINKLED* family (*WRI5a–WRI5c*); the latter directly regulate expression of lipid biosynthesis genes (Park et al., 2015; Luginbuehl et al., 2017; Jiang et al., 2018). We found that *BdRAD1* and the three *B. distachyon* AP2 family transcription factors most closely related to *MtWRI5a* to *MtWRI5c* (further denoted as *BdWRI5.1*, *BdWRI5.2*, and *BdWRI5.3*) were strongly induced in wild-type roots colonized with *D. epigaea* relative to mock-inoculated controls (Supplemental Fig. S3), but interestingly, only *BdWRI5.1* was induced in noncolonized *35S:BdRAM1^{ox}* roots (Fig. 3B). A similar pattern was observed in *35S:BdRAM1^{ox}* shoots (Fig. 4B; Supplemental Fig. S5). Thus, in contrast to *M. truncatula*, a RAM1-independent pathway likely leads to up-regulation of *BdRAD1*, *BdWRI5.2*, and *BdWRI5.3* in mycorrhizal roots. This points to functional diversification of the regulatory cascade responsible for the transcriptional reprogramming of roots during AM symbiosis in *B. distachyon*. In addition, it may provide an explanation for the relatively mild *ram1* mutant phenotype we observed (Fig. 2). Future research in other monocot species is required to determine if such a functional diversification is unique to *B. distachyon* or a monocot-specific phenomenon.

Arbuscule Density Is Higher in *RAM1* Overexpressors Relative to Controls

The initial goal of this study was to test the hypothesis that constitutive overexpression of *RAM1* would increase arbuscule density and/or colonization and

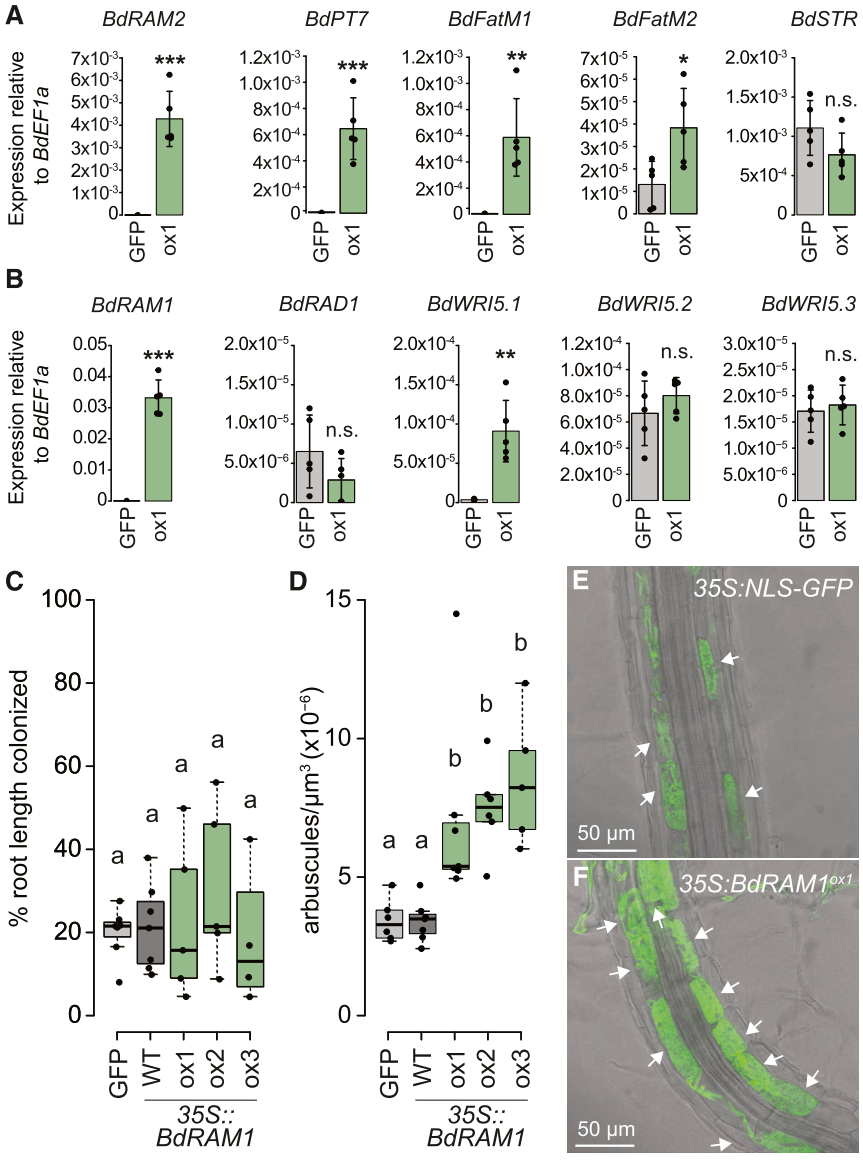

Figure 3. Ectopic overexpression of *BdRAM1* promotes arbuscule formation and expression of AM marker genes. A, Gene expression levels of *B. distachyon* orthologs of *MtRAM1* target genes in noncolonized *35S:NLS-GFP* (denoted as GFP) and *35S:BdRAM1^{ox}* line 1 (denoted as ox1) roots. *35S:BdRAM1^{ox}* roots display induced expression of *BdRAM1*, as well as *BdRAM2*, *BdPT7*, *BdFatM1*, and *BdFatM2* in the absence of symbiosis relative to *35S:NLS-GFP* control roots. *BdSTR* gene expression is not affected in these roots. B, Gene expression of *B. distachyon RAD1* and *WRI5* orthologs. Only expression of *BdWRI5.1* is induced in noncolonized *35S:BdRAM1^{ox}* roots relative to *35S:NLS-GFP* control roots. A and B, Bar graphs show the mean, with error bars representing SD. Single points represent individual measurements. Pairwise comparisons were estimated using the Student's *t* test (***$P < 0.001$, **$P < 0.01$, and *$P < 0.05$).; n.s., Not significant. C, Quantification of total root colonization in independent lines transformed with *35S:BdRAM1*. There is no difference in overall root colonization between three lines ectopically overexpressing *35S:BdRAM1* (*35S:BdRAM1^{ox}*, denoted as ox1, ox2, and ox3) and control plants (*35S:BdRAM1^{WT}*, which does not overexpress *BdRAM1* and was therefore denoted as WT [wild type]; and *35S:NLS-GFP*, labeled as GFP). ANOVA ($P = 0.71$). Root-length colonization was quantified using the grid-line method (McGonigle et al., 1990). D, Quantification of *D. epigaea* arbuscules in a defined area at the fungal hyphopodium. Roots of three independent transgenic *35S:BdRAM1^{ox}* lines (denoted as ox1, ox2, and ox3) contain more arbuscules than roots transformed with the control construct *35S:NLS-GFP* (GFP) or roots that contain *35S:BdRAM1* but do not overexpress the gene (WT). Arbuscule number was normalized to the volume of the confocal stack. Kruskal-Wallis test ($P = 1.32 \times 10^{-4}$), pairwise comparisons were conducted using the Dunn's post-hoc test. Different lowercase letters denote significant differences. Box and whisker plots show lower and upper quartiles and minimum and maximum values. The horizontal bar represents the median and the points individual measurements. E, Representative image of a *35S:NLS-GFP* root colonized by *D. epigaea*. F, Representative image of a *RAM1*-overexpressing *35S:BdRAM1^{ox}* (line 1) root colonized by *D. epigaea*. In E and F, arbuscules are highlighted with arrows.

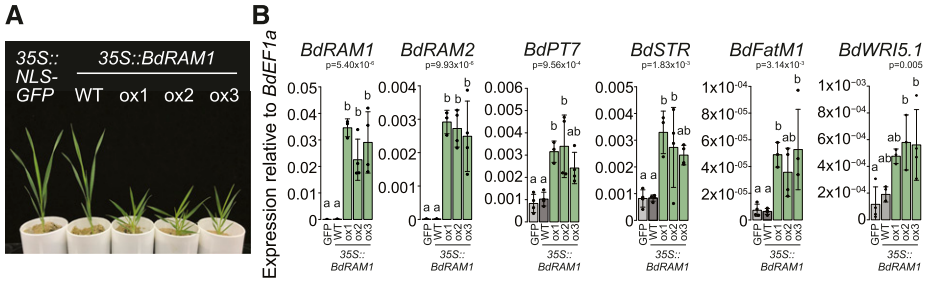

Figure 4. *RAM1* overexpressors show altered shoot development and constitutively express root AM marker genes in their shoots. A, Photograph of 4.5-week-old *B. distachyon* plants transformed with *35S:NLS-GFP* or *35S:BdRAM1*. The three independent transformant lines overexpressing *BdRAM1* (ox1, ox2, and ox3) display a bushy stature, whereas the *35S:BdRAM1*-transformant line not overexpressing *BdRAM1* (wild type [WT]) resembles the *35S:NLS-GFP* control plant. B, Gene expression of *BdRAM1* and of several root AM marker genes in shoots. All tested genes are strongly induced in 4.5-week-old shoots of three *35S:BdRAM1^{ox}* lines (ox1, ox2, and ox3) relative to control plants transformed with *35S:NLS-GFP* (GFP) or the *35S:BdRAM1*-transformant line not overexpressing *BdRAM1* (wild type). Gene expression was measured by RT-qPCR. Bar graphs show the mean, with error bars representing SD. Single points represent individual measurements. Significance values (ANOVA) for each gene are indicated in the figure. Pairwise comparisons were conducted using Tukey's HSD post-hoc test. Different lowercase letters denote significant differences.

then to use the plants to address secondary hypotheses about symbiotic performance.

To test the first hypothesis, we grew *35S:BdRAM1^{ox}*, *35S:BdRAM1^{WT}*, and *35S:NLS-GFP* control plants in substrate containing *D. epigaea* spores and evaluated colonization levels and arbuscule morphology. Colonization levels in *35S:BdRAM1^{ox}* and control plants did not differ significantly, although the variation was much greater in the *35S:BdRAM1^{ox}* plants (Fig. 3C). Arbuscules in *35S:BdRAM1^{ox}* plants showed a wild-type morphology, but the number of arbuscules, which we assessed within a defined root volume below the hyphopodium, was on average 2-fold greater in the *35S:BdRAM^{ox}* plants relative to controls (Fig. 3, D–F; Supplemental Fig. S5). Thus, *35S:BdRAM1^{ox}* plants have a higher capacity to establish and/or to maintain arbuscules relative to the control plants. As RAM1 regulates the expression of several other transcription factors, as well as genes involved in lipid biosynthesis and nutrient transport, the increased arbuscule density in the *35S:BdRAM1^{ox}* plants may result from a combination of factors including arbuscule initiation and/or regulation of arbuscule lifespan.

Unfortunately, the severe shoot growth and branching phenotype of the *BdRAM1* overexpressors prevented a fair evaluation of symbiotic performance (Supplemental Fig. S5). While colonized *35S:BdRAM1^{ox}* plants and controls both showed an increase in shoot fresh weight and tiller number relative to their respective mock-inoculated controls, the differences in the developmental architecture of these lines precluded direct physiological comparisons. Consequently, it was not possible to determine whether the increased arbuscule density influenced symbiotic performance.

Hormone Biosynthetic and Regulatory Gene Expression Is Altered in *BdRAM1* Overexpressors

The shoot architecture phenotype of the *35S:BdRAM1^{ox}* plants is reminiscent of the phenotypes of several monocot hormone mutants. For example, rice and *B. distachyon*

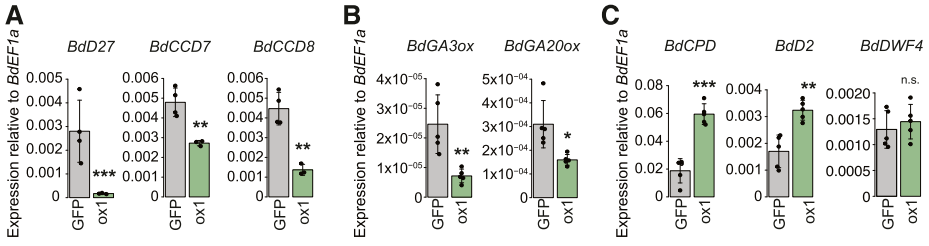

Figure 5. Expression of hormone biosynthesis genes is altered in roots of *RAM1* overexpressors. A, *B. distachyon* orthologs of three genes involved in the SL biosynthesis pathway (*BdD27*, *BdCCD7*, and *BdCCD8*) are down-regulated in noncolonized roots ectopically overexpressing *BdRAM1* (*35S:BdRAM1^{ox}* line 1, denoted as ox1) relative to *35S:NLS-GFP* ("GFP") control roots. B, Two genes with a putative function in GA biosynthesis (*BdGA3ox1* and *BdGA20ox1*) are down-regulated in *35S:BdRAM1^{ox}* roots. C, Two *B. distachyon* genes orthologous to known brassinosteroid biosynthesis genes (*BdCPD* and *BdD2/BdCYP91D*) are induced in *35S:BdRAM1^{ox}* roots. A third gene, *BdDWF4*, is not affected. Gene expression was measured by RT-qPCR. Bar graphs show the mean, with error bars representing SD. Single points represent individual measurements. Pairwise comparisons were estimated using the Student's *t* test (***$P < 0.001$, **$P < 0.01$, and *$P < 0.05$). n.s., Not significant.

mutants defective in GA, SL, and brassinosteroid (BR) biosynthesis or signaling display dwarf phenotypes with increased tillering (e.g. Spielmeyer et al., 2002; Ishikawa et al., 2005; Asano et al., 2009; Lin et al., 2009; Thole et al., 2012). To obtain further clues about the *BdRAM1* overexpression phenotype, we evaluated the expression of several genes associated with SL, GA, and BR signaling. *B. distachyon* orthologs of genes involved in SL biosynthesis (*BdD27*, *BdCCD7*, and *BdCCD8*; Seto and Yamaguchi, 2014) and GA biosynthesis (potential orthologs of Arabidopsis [*Arabidopsis thaliana*] *GA3ox1* and *GA20ox1*; Kakei et al., 2015) were down-regulated, while key BR biosynthesis genes (*BdCPD* and *BdD2/CYP90D*) but not *BdDWF4* (Kakei et al., 2015) were elevated in noncolonized *35S:BdRAM1^{ox}* roots relative to the controls (Fig. 5). The GA receptor *GID1* and the GA regulator *DELLA/SLR1* (Davière and Achard, 2013) as well as the regulators of SL signaling *D3* and *D53* (Seto and Yamaguchi, 2014), and the *B. distachyon* BR receptor *BdBRI1* and the BR-responsive transcription factor *BdBZR1* (Corvalán and Choe, 2017) were differentially regulated in *35S:BdRAM1^{ox}* roots relative to controls (Supplemental Fig. S6). In addition, altered expression of some BR biosynthesis genes and GA biosynthesis and signaling genes was observed in *35S:BdRAM1^{ox}* shoots (Supplemental Table S1). Thus, the transcript data indicate a disturbance in hormone biosynthetic and regulatory gene expression likely contributing to the altered shoot architecture. Because of substantial cross talk between hormone signaling pathways (Itoh et al., 2001; Umehara et al., 2008; Unterholzner et al., 2015; Corvalán and Choe, 2017), it is not possible to predict the initial cause. As GA, SL, and BR hormone pathways each involve regulation via GRAS transcription factors (Tong et al., 2009; Liu et al., 2011; Chen et al., 2013), it is possible that ectopic overexpression of *BdRAM1* disturbs GRAS-factor complexes, leading to misregulation of these pathways. Alternatively, one of the native functions of *BdRAM1* may be to regulate aspects of hormone signaling. For example, in rice, RAM1 interacts with a DELLA-interacting protein (DIP), and therefore it is possible that one of RAM1's native functions is to influence GA signaling and that this is exacerbated in the *35S:BdRAM1^{ox}* line, leading to further downstream effects on other pathways. SL promotes initiation of AM symbiosis, influencing both primary and secondary infections, and BR is a positive regulator of AM symbiosis in some plant species (for review, see Kobae et al., 2018; Liao et al., 2018; Müller and Harrison, 2019); however, direct effects on arbuscule development have not been reported for these hormones. By contrast, it is well established that GA is involved in arbuscule formation and regulation of arbuscule lifespan (Floss et al., 2013, 2017; Yu et al., 2014). If misregulation of GA biosynthesis gene expression translates to disturbed GA homeostasis in *35S:BdRAM1^{ox}* roots, an imbalance in GA-regulated arbuscule formation and degradation could result (Floss et al., 2013, 2017). Such a scenario might explain the increased arbuscule numbers in *35S:BdRAM1^{ox}* roots as well as a dwarf shoot phenotype.

CONCLUSION

In conclusion, *BdRAM1*, similar to its orthologs in dicots, regulates arbuscule development and transcriptional regulation of several AM symbiosis-induced genes, although it is likely that there is some functional redundancy with other GRAS or WRI5 transcription factors. Constitutive overexpression of *35S:BdRAM1* increased arbuscule density relative to control plants; although the plants were unsuitable for experiments to assess the functional consequences of increasing the symbiotic interfaces, the data nevertheless indicate that it is possible to manipulate arbuscule density through expression of *RAM1*. Whether this is a direct effect via elevated expression of known *BdRAM1* target genes or an indirect effect through phytohormones that influence plant architecture as well as arbuscule initiation, development, or lifespan is currently unknown.

Future research should focus on increasing *RAM1* gene expression specifically in the root cortex. We predict such a strategy would increase arbuscule density without the accompanying developmental defects and would enable evaluation of the consequences of increasing the density of symbiotic interfaces and the effects on nutrient exchange during AM symbiosis.

MATERIALS AND METHODS

Plant Material and Growth Conditions

Brachypodium distachyon plants were grown in a growth chamber under a 12-h light (24°C)/12-h dark (22°C) regime. For all experiments that were conducted in the absence of an AM fungal symbiont, *B. distachyon* plants were grown in 20.5-cm-long cones filled with sterile Terragreen (Oli-Dri) and play sand (Quikrete) in a ratio of 1:1. For all experiments involving AM symbiosis, *B. distachyon* plants were grown in cones filled with a sand-gravel mix and were inoculated with 250 *Diversispora epigaea* spores (formerly *Glomus versiforme*) as previously described (Müller et al., 2019). For mock-inoculated controls, we added an appropriate volume of filtered spore wash solution instead of the spores. Unless otherwise stated, *B. distachyon* plants were fertilized once per week with one-fourth-strength Hoagland's fertilizer containing 20 μM Pi and harvested 4 to 5 weeks after transplanting to cones.

To monitor AM growth responses, seedlings were planted into pots (three seedlings per 11-cm-diameter pot and eight pots per genotype) containing a 1:20 mixture of autoclaved N7/N8 soil (Watts-Williams et al., 2019) to sand/gravel mix. The sand/gravel mix is a 2:2:1 mixture of play sand, fine black sand, and gravel as described in Floss et al. (2017). Two hundred fifty surface-sterilized *D. epigaea* spores were placed below each plant. Beginning at 3 weeks postplanting, the pots were fertilized weekly with 50 mL of one-fourth-strength Hoagland's solution lacking phosphate and 9 mL of 0.5 mM $Ca_3(PO_4)_2$. Plants were harvested at 9 weeks postplanting. The growth chamber conditions were as described above.

Plasmid Generation

To clone the CRISPR/Cas9 construct targeting *BdRAM1*, we used the vector and cloning system described previously (Xie et al., 2015). To design the primers (shown in Supplemental Table S2), gene-specific guide RNA sequences targeting *Bradi4g18390* were identified using CRISPR-P (Lei et al., 2014) and CRISPR-PLANT (Xie et al., 2015) and selected based on their location in the coding sequence and low number of off-target sites. We generated a two-guide

CRISPR/Cas9 construct that targeted *Bradi4g18390* at positions 32 to 54 bp (guide RNA1) and 280 to 302 bp (guide RNA2) downstream of the transcription start site (Supplemental Fig. S2). As a negative control, we used the empty vector *pRGEB32* (Xie et al., 2015).

To clone *35S:BdRAM1* overexpression constructs, the coding sequence of *Bradi4g18390* was amplified using gene-specific primers flanked by *att*B1 and *att*B2 recombination sites (Supplemental Table S2) and cloned into *pDONR221*, resulting in the *pENTR1-2 BdRAM1* entry clone. *pENTR1-2* clones containing the coding sequence of *NLS-GFP-GUS*, as well as *pENTR4-1* entry clones containing the *CaMV35S* promoter and *pENTR2-3* containing the *CaMV35S* terminator were cloned previously (Ivanov and Harrison, 2014; Floss et al., 2017). To assemble the binary vectors for *B. distachyon* transformation, four vectors (*pENTR4-1* containing the double *CaMV35S* promoter, *pENTR1-2* containing *BdRAM1* or *NLS-GFP-GUS*, *pENTR2-3* containing the *CaMV35S* terminator, and *pHb7m34GW*; Karimi et al., 2005) were combined to generate *35S:BdRAM1* or *35S:NLS-GFP* using the multisite gateway cloning system (Invitrogen). All vector sequences were confirmed by Sanger sequencing.

Generation of *B. distachyon* Transformants

The CRISPR/Cas9 constructs targeting *BdRAM1* as well as the *35S:BdRAM1* and *35S:NLS-GFP* constructs were transformed into *B. distachyon* (accession Bd21-3) following a previously established protocol (Bragg et al., 2015). Plantlets emerging from transformed calli (selectable marker, hygromycin) were transplanted into Metro-Mix 350 and genotyped to test for the presence of the construct (see Supplemental Table S2 for primer sequences). In addition, in the case of the CRISPR/Cas9 constructs, the CRISPR/Cas9 target loci were amplified using flanking primers, and purified PCR products were Sanger sequenced in order to identify gene edits.

Visualization and Quantification of Fungal Root Colonization

Fungal colonization of *B. distachyon* roots was visualized by staining with wheat-germ agglutinin coupled to Alexa Fluor 488 as previously described (Hong et al., 2012). Roots were observed using a Leica M205 stereomicroscope, and root colonization was quantified using the gridline-intersect method (McGonigle et al., 1990). To quantify the *ram1* phenotype, roots intersecting the gridlines were scored into one of three categories: (1) not colonized; (2) colonized with wild type-like arbuscules; and (3) colonized with aberrant (sparsely branched or collapsed arbuscules) or no arbuscules. The ratio of category 3 over the overall number of intersections of colonized roots (category $2 + 3) \times 100$ was used to determine the percentage of intersections without arbuscules/total colonization. Total root-length colonization was calculated as the percentage of category $2 + 3$ over the total number of intersections counted $\times$ 100. To study arbuscule morphology, wheat-germ agglutinin-Alexa Fluor 488-stained roots were counterstained with propidium iodide to visualize plant cell walls and observed with a Leica SP5 confocal microscope. To quantify arbuscule numbers in *35S:BdRAM1^{ox}* roots, confocal stacks from highly colonized roots were taken so that the fungal hyphopodium was in the center of the image to ensure we captured infections of similar developmental stages. The total number of arbuscules per stack was assessed manually using the Fiji image analysis package (Schindelin et al., 2012). Stack depth (z plane) was chosen to encompass the whole infection, and arbuscule numbers were normalized against the stack volume (length of $x \times y \times z$ planes). To avoid potentially confounding effects caused by different *B. distachyon* root types, we selected only thin lateral roots with a single layer of cortical cells for analysis.

RNA Isolation, cDNA Synthesis, and RT-qPCR

RNA isolation, cDNA synthesis, and RT-qPCR were performed as previously described (Müller et al., 2019). Primers used to quantify expression of target genes are shown in Supplemental Table S2. Ct values of the tested genes were normalized against *BdEF1α* (resulting in ΔCt), and relative expression levels were calculated with the equation $2^{-\Delta Ct}$.

Assessment of Plant Morphology

Plants were grown in the absence of AM fungi, and whole plants were harvested 2, 4, and 6 weeks after planting. Tiller and node root numbers were counted, and maximal root system and shoot length were measured. The angle between individual leaves and the stem was measured on images of the same plants using the Fiji image analysis package (Schindelin et al., 2012).

Phylogenetic Analyses

B. distachyon orthologs of *Medicago truncatula* RAM1, RAD1, RAM2, PT4, FatM, STR, and WRI5a to WRI5c as well as *Oryza sativa* D27, D17/CCD7, D10/CCD8, D3, D53, D14, D14L, and SLR1 were identified using phylogenetic approaches described previously (Supplemental Figs. S1 and S7; Bravo et al., 2016). *B. distachyon* genes putatively involved in BR and GA biosynthesis and signaling were identified previously (Kakei et al., 2015; Corvalán and Choe, 2017; Niu et al., 2019).

Statistical Analyses and Data Representation

All experiments were performed using three to 10 biological replicates. All experiments were repeated at least two times. The distribution of residuals was tested for normality using the Shapiro-Wilk test. If normality assumption was met, pairwise comparisons were analyzed using a two-sided Student's *t* test. For multiple comparisons, the raw data were subjected to a one-way ANOVA followed by Tukey's post-hoc test. If normality assumption was not met, data were analyzed using the Kruskal-Wallis test followed by Dunn's post-hoc test (*P* values adjusted after Benjamini-Hochberg). All statistical analyses were performed using R software. Quantification data for $n > 5$ biological replicates are represented as box and whisker plots, which show the lower and upper quartiles as well as the minimum and maximum values. The horizontal line in the box plots represents the median. Points represent single measurements. For datasets with less than five measurements per genotype, bar plots were chosen. Bars represent the mean and error bars the SD. Points represent single measurements.

Accession Numbers

B. distachyon gene identifiers for all genes referred to in this manuscript can be found in Supplemental Table S2.

Supplemental Data

The following materials are available.

Supplemental Figure S1. Phylogenetic tree showing GRAS transcription factors related to *Bd*RAM1 in the AM host species (*B. distachyon*, *O. sativa*, *Hordeum vulgare*, *Zea mays*, *M. truncatula*) and the nonhost species Arabidopsis.

Supplemental Figure S2. *B. distachyon* CRISPR/Cas9 edited *ram1* mutants.

Supplemental Figure S3. Gene expression of selected AM marker genes in colonized roots.

Supplemental Figure S4. Developmental phenotypes caused by ectopic overexpression of *BdRAM1* measured at 2, 4, and 6 weeks postplanting.

Supplemental Figure S5. Growth response experiment and analysis of arbuscule numbers and gene expression in *35S:BdRAM1ox* plants.

Supplemental Figure S6. Ectopic overexpression of *BdRAM1* influences expression of genes associated with SL, GA, and BR signaling.

Supplemental Figure S7. Phylogenetic trees used to identify *B. distachyon* orthologs of AM marker genes.

Supplemental Table S1. Gene expression fold change of selected hormone marker genes in shoots overexpressing *BdRAM1*.

Supplemental Table S2. Primers used in this study.

ACKNOWLEDGMENTS

We thank Sophia Cotraccia, Cassandra Proctor, and Stephanie Roh for technical assistance and the Boyce Thompson Institute Biotechnology Center for generating some of the *B. distachyon* transgenic lines.

Received July 28, 2020; accepted August 20, 2020; published September 1, 2020.

LITERATURE CITED

Asano K, Hirano K, Ueguchi-Tanaka M, Angeles-Shim RB, Komura T, Satoh H, Kitano H, Matsuoka M, Ashikari M (2009) Isolation and characterization of dominant dwarf mutants, Slr1-d, in rice. Mol Genet Genomics **281:** 223–231

Bragg JN, Anderton A, Nieu R, Vogel JP (2015) *Brachypodium distachyon*. Methods Mol Biol **1223:** 17–33

Bravo A, Brands M, Wewer V, Dörmann P, Harrison MJ (2017) Arbuscular mycorrhiza-specific enzymes FatM and RAM2 fine-tune lipid biosynthesis to promote development of arbuscular mycorrhiza. New Phytol **214:** 1631–1645

Bravo A, York T, Pumplin N, Mueller LA, Harrison MJ (2016) Genes conserved for arbuscular mycorrhizal symbiosis identified through phylogenomics. Nat Plants **2:** 15208

Cenci A, Rouard M (2017) Evolutionary analyses of GRAS transcription factors in angiosperms. Front Plant Sci **8:** 273

Chen L, Xiong G, Cui X, Yan M, Xu T, Qian Q, Xue Y, Li J, Wang Y (2013) OsGRAS19 may be a novel component involved in the brassinosteroid signaling pathway in rice. Mol Plant **6:** 988–991

Corvalán C, Choe S (2017) Identification of brassinosteroid genes in *Brachypodium distachyon*. BMC Plant Biol **17:** 5

Davière JM, Achard P (2013) Gibberellin signaling in plants. Development **140:** 1147–1151

Floss DS, Gomez SK, Park HJ, MacLean AM, Müller LM, Bhattarai KK, Lévesque-Tremblay V, Maldonado-Mendoza IE, Harrison MJ (2017) A transcriptional program for arbuscule degeneration during AM symbiosis is regulated by MYB1. Curr Biol **27:** 1206–1212

Floss DS, Lévesque-Tremblay V, Park HJ, Harrison MJ (2016) DELLA proteins regulate expression of a subset of AM symbiosis-induced genes in *Medicago truncatula*. Plant Signal Behav **11:** e1162369

Floss DS, Levy JG, Levesque-Tremblay V, Pumplin N, Harrison MJ (2013) DELLA proteins regulate arbuscule formation in arbuscular mycorrhizal symbiosis. Proc Natl Acad Sci USA **110:** E5025–E5034

Fonouni-Farde C, Tan S, Baudin M, Brault M, Wen J, Mysore KS, Niebel A, Frugier F, Diet A (2016) DELLA-mediated gibberellin signalling regulates Nod factor signalling and rhizobial infection. Nat Commun **7:** 12636

Foo E, Ross JJ, Jones WT, Reid JB (2013) Plant hormones in arbuscular mycorrhizal symbioses: An emerging role for gibberellins. Ann Bot **111:** 769–779

Gobbato E, Marsh JF, Vernié T, Wang E, Maillet F, Kim J, Miller JB, Sun J, Bano SA, Ratet P, et al (2012) A GRAS-type transcription factor with a specific function in mycorrhizal signaling. Curr Biol **22:** 2236–2241

Gobbato E, Wang E, Higgins G, Bano SA, Henry C, Schultze M, Oldroyd GED (2013) RAM1 and RAM2 function and expression during arbuscular mycorrhizal symbiosis and *Aphanomyces euteiches* colonization. Plant Signal Behav **8:** e26049

Gomez-Roldan V, Fermas S, Brewer PB, Puech-Pagès V, Dun EA, Pillot J-P, Letisse F, Matusova R, Danoun S, Portais J-C, et al (2008) Strigolactone inhibition of shoot branching. Nature **455:** 189–194

Gutjahr C, Banba M, Croset V, An K, Miyao A, An G, Hirochika H, Imaizumi-Anraku H, Paszkowski U (2008) Arbuscular mycorrhiza-specific signaling in rice transcends the common symbiosis signaling pathway. Plant Cell **20:** 2989–3005

Gutjahr C, Radovanovic D, Geoffroy J, Zhang Q, Siegler H, Chiapello M, Casieri L, An K, An G, Guiderdoni E, et al (2012) The half-size ABC transporters STR1 and STR2 are indispensable for mycorrhizal arbuscule formation in rice. Plant J **69:** 906–920

Harrison MJ, Dewbre GR, Liu J (2002) A phosphate transporter from *Medicago truncatula* involved in the acquisition of phosphate released by arbuscular mycorrhizal fungi. Plant Cell **14:** 2413–2429

Heck C, Kuhn H, Heidt S, Walter S, Rieger N, Requena N (2016) Symbiotic fungi control plant root cortex development through the novel GRAS transcription factor MIG1. Curr Biol **26:** 2770–2778

Hong JJ, Park YS, Bravo A, Bhattarai KK, Daniels DA, Harrison MJ (2012) Diversity of morphology and function in arbuscular mycorrhizal symbioses in *Brachypodium distachyon*. Planta **236:** 851–865

Ishikawa S, Maekawa M, Arite T, Onishi K, Takamure I, Kyozuka J (2005) Suppression of tiller bud activity in tillering dwarf mutants of rice. Plant Cell Physiol **46:** 79–86

Itoh H, Ueguchi-Tanaka M, Sentoku N, Kitano H, Matsuoka M, Kobayashi M (2001) Cloning and functional analysis of two gibberellin 3 beta-hydroxylase genes that are differently expressed during the growth of rice. Proc Natl Acad Sci USA **98:** 8909–8914

Ivanov S, Harrison MJ (2014) A set of fluorescent protein-based markers expressed from constitutive and arbuscular mycorrhiza-inducible promoters to label organelles, membranes and cytoskeletal elements in *Medicago truncatula*. Plant J **80:** 1151–1163

Jiang Y, Wang W, Xie Q, Liu N, Liu L, Wang D, Zhang X, Yang C, Chen X, Tang D, et al (2017) Plants transfer lipids to sustain colonization by mutualistic mycorrhizal and parasitic fungi. Science **356:** 1172–1175

Jiang Y, Xie Q, Wang W, Yang J, Zhang X, Yu N, Zhou Y, Wang E (2018) Medicago AP2-domain transcription factor WRI5a is a master regulator of lipid biosynthesis and transfer during mycorrhizal symbiosis. Mol Plant **11:** 1344–1359

Jin Y, Liu H, Luo D, Yu N, Dong W, Wang C, Zhang X, Dai H, Yang J, Wang E (2016) DELLA proteins are common components of symbiotic rhizobial and mycorrhizal signalling pathways. Nat Commun **7:** 12433

Kakei Y, Mochida K, Sakurai T, Yoshida T, Shinozaki K, Shimada Y (2015) Transcriptome analysis of hormone-induced gene expression in *Brachypodium distachyon*. Sci Rep **5:** 14476

Karimi M, De Meyer B, Hilson P (2005) Modular cloning in plant cells. Trends Plant Sci **10:** 103–105

Kobae Y, Kameoka H, Sugimura Y, Saito K, Ohtomo R, Fujiwara T, Kyozuka J (2018) Strigolactone biosynthesis genes of rice are required for the punctual entry of arbuscular mycorrhizal fungi into the roots. Plant Cell Physiol **59:** 544–553

Lei Y, Lu L, Liu H-Y, Li S, Xing F, Chen L-L (2014) CRISPR-P: A web tool for synthetic single-guide RNA design of CRISPR-system in plants. Mol Plant **7:** 1494–1496

Liao D, Wang S, Cui M, Liu J, Chen A, Xu G (2018) Phytohormones regulate the development of arbuscular mycorrhizal symbiosis. Int J Mol Sci **19:** 3146

Lin H, Wang R, Qian Q, Yan M, Meng X, Fu Z, Yan C, Jiang B, Su Z, Li J, et al (2009) DWARF27, an iron-containing protein required for the biosynthesis of strigolactones, regulates rice tiller bud outgrowth. Plant Cell **21:** 1512–1525

Liu W, Kohlen W, Lillo A, Op den Camp R, Ivanov S, Hartog M, Limpens E, Jamil M, Smaczniak C, Kaufmann K, et al (2011) Strigolactone biosynthesis in *Medicago truncatula* and rice requires the symbiotic GRAS-type transcription factors NSP1 and NSP2. Plant Cell **23:** 3853–3865

Luginbuehl LH, Menard GN, Kurup S, Van Erp H, Radhakrishnan GV, Breakspear A, Oldroyd GED, Eastmond PJ (2017) Fatty acids in arbuscular mycorrhizal fungi are synthesized by the host plant. Science **356:** 1175–1178

McGonigle TP, Miller MH, Evans DG, Fairchild GL, Swan JA (1990) A new method which gives an objective measure of colonization of roots by vesicular-arbuscular mycorrhizal fungi. New Phytol **115:** 495–501

Müller LM, Flokova K, Schnabel E, Sun X, Fei Z, Frugoli J, Bouwmeester HJ, Harrison MJ (2019) A CLE-SUNN module regulates strigolactone content and fungal colonization in arbuscular mycorrhiza. Nat Plants **5:** 933–939

Müller LM, Harrison MJ (2019) Phytohormones, miRNAs, and peptide signals integrate plant phosphorus status with arbuscular mycorrhizal symbiosis. Curr Opin Plant Biol **50:** 132–139

Niu X, Chen S, Li J, Liu Y, Ji W, Li H (2019) Genome-wide identification of GRAS genes in *Brachypodium distachyon* and functional characterization of BdSLR1 and BdSLRL1. BMC Genomics **20:** 635

Park HJ, Floss DS, Levesque-Tremblay V, Bravo A, Harrison MJ (2015) Hyphal branching during arbuscule development requires Reduced Arbuscular Mycorrhiza1. Plant Physiol **169:** 2774–2788

Paszkowski U, Kroken S, Roux C, Briggs SP (2002) Rice phosphate transporters include an evolutionarily divergent gene specifically activated in arbuscular mycorrhizal symbiosis. Proc Natl Acad Sci USA **99:** 13324–13329

Pimprikar P, Carbonnel S, Paries M, Katzer K, Klingl V, Bohmer MJ, Karl L, Floss DS, Harrison MJ, Parniske M, et al (2016) A CCaMK-CYCLOPS-DELLA complex activates transcription of *RAM1* to regulate arbuscule branching. Curr Biol **26:** 987–998

Pimprikar P, Gutjahr C (2018) Transcriptional regulation of arbuscular mycorrhiza development. Plant Cell Physiol **59:** 673–690

Rich MK, Courty PE, Roux C, Reinhardt D (2017) Role of the GRAS transcription factor ATA/RAM1 in the transcriptional reprogramming of arbuscular mycorrhiza in *Petunia hybrida*. BMC Genomics **18:** 589

Rich MK, Schorderet M, Bapaume L, Falquet L, Morel P, Vandenbussche M, Reinhardt D (2015) The Petunia GRAS transcription factor ATA/RAM1 regulates symbiotic gene expression and fungal morphogenesis in arbuscular mycorrhiza. Plant Physiol **168:** 788–797

Schindelin J, Arganda-Carreras I, Frise E, Kaynig V, Longair M, Pietzsch T, Preibisch S, Rueden C, Saalfeld S, Schmid B, et al (2012) Fiji: An open-source platform for biological-image analysis. Nat Methods **9:** 676–682

Seto Y, Yamaguchi S (2014) Strigolactone biosynthesis and perception. Curr Opin Plant Biol **21:** 1–6

Spielmeyer W, Ellis MH, Chandler PM (2002) Semidwarf (sd-1), "green revolution" rice, contains a defective gibberellin 20-oxidase gene. Proc Natl Acad Sci USA **99:** 9043–9048

Thole V, Peraldi A, Worland B, Nicholson P, Doonan JH, Vain P (2012) T-DNA mutagenesis in *Brachypodium distachyon*. J Exp Bot **63:** 567–576

Tong H, Jin Y, Liu W, Li F, Fang J, Yin Y, Qian Q, Zhu L, Chu C (2009) DWARF AND LOW-TILLERING, a new member of the GRAS family, plays positive roles in brassinosteroid signaling in rice. Plant J **58:** 803–816

Umehara M, Hanada A, Yoshida S, Akiyama K, Arite T, Takeda-Kamiya N, Magome H, Kamiya Y, Shirasu K, Yoneyama K, et al (2008) Inhibition of shoot branching by new terpenoid plant hormones. Nature **455:** 195–200

Unterholzner SJ, Rozhon W, Papacek M, Ciomas J, Lange T, Kugler KG, Mayer KF, Sieberer T, Poppenberger B (2015) Brassinosteroids are master regulators of gibberellin biosynthesis in Arabidopsis. Plant Cell **27:** 2261–2272

Watts-Williams SJ, Emmett BD, Levesque-Tremblay V, MacLean AM, Sun X, Satterlee JW, Fei Z, Harrison MJ (2019) Diverse *Sorghum bicolor* accessions show marked variation in growth and transcriptional responses to arbuscular mycorrhizal fungi. Plant Cell Environ **42:** 1758–1774

Xie K, Minkenberg B, Yang Y (2015) Boosting CRISPR/Cas9 multiplex editing capability with the endogenous tRNA-processing system. Proc Natl Acad Sci USA **112:** 3570–3575

Xue L, Cui H, Buer B, Vijayakumar V, Delaux P-M, Junkermann S, Bucher M (2015) Network of GRAS transcription factors involved in the control of arbuscule development in *Lotus japonicus*. Plant Physiol **167:** 854–871

Yu N, Luo D, Zhang X, Liu J, Wang W, Jin Y, Dong W, Liu J, Liu H, Yang W, et al (2014) A DELLA protein complex controls the arbuscular mycorrhizal symbiosis in plants. Cell Res **24:** 130–133

Zhang Q, Blaylock LA, Harrison MJ (2010) Two *Medicago truncatula* half-ABC transporters are essential for arbuscule development in arbuscular mycorrhizal symbiosis. Plant Cell **22:** 1483–1497